Investigation on optoelectronic and thermoelectric characteristics of half-Heusler compound RbSrBi: A first-principles study

Roll: 191314
Session: 2019–2020

Report submitted to the Department of Physics at
Jashore University of Science and Technology
in partial fulfillment of the requirements
for the degree of Bachelor of Science
with Honours in Physics

May 2025

Abstract

The objective of the current study is to investigate the structural, optoelectronic, and thermoelectric characteristics of RbSrBi half-Heusler compound. The structural, optoelectronic, and thermoelectric characteristics of RbSrBi half-Heusler are studied utilizing the full potential linearized augmented plane wave programs (FP-LAPW) approach as embedded in WIEN2k. Structural optimization was performed using Perdew-Burke-Ernzerhof Generalized Gradient Approximation (PBE-GGA). The RbSrBi compound shows semiconducting behavior with a direct bandgap. The computed band gap for RbSrBi is 1.583 eV using the Tran-Blaha modified Becke-Johnson (TB-mBJ) approximation. Analysis of the calculated band structure, density of states and optical spectra reveal the material's capability to absorb ultraviolet and visible light. The exploration of thermoelectric properties was calculated using the BoltzTraP code. Around room temperature, the obtained figures of merit (ZT) value for the compound is very close to unity, indicating the potential for thermoelectric devices designed with the materials to achieve maximum thermoelectric efficiency.

Acknowledgements

First of all, I praise and thank Almighty Allah, the Lord of the worlds, the Most Merciful, the Guider of hearts, the Provider of sustenance, the Owner of life and death.

I would like to thank my supervisor, Dr. Mohammad Abdur Rashid, for his constant support and guidance to complete my project work properly. During the period of this project, he always shows me invaluable confidence. He taught me how to precisely calculate all the characteristics and provided a wealth of knowledge that helped me produce an appropriate project report. I want to express my gratitude to the Quantum Materials Simulation Lab (QMSL) members who supported me throughout the project, both directly and indirectly. They are helpful and amicable. In addition, QMSL has provided me with several facilities, including enough computational support, printing facilities, a comfortable workstation and so on.

On a personal note, I would like to thank my respectable parents for their sacrifice and support over the years. Their love and encouragement always give me mental support to continue my study smoothly.

Contents

Investigation on optoelectronic and thermoelectric characteristics of half-Heusler compound RbSrBi: A first-principles study

1 Introduction **1**

2 Theoretical background **4**

2.1 Basic Quantum Mechanics 5

2.1.1 Schrödinger Equation 5

2.1.2 Wave Functions and Probability Density 6

2.2 The Many-Body Problem 6

2.2.1 Born-Oppenheimer Approximation 8

2.2.2 Hartree-Fock Approximation and Its Limitations 10

2.3 Density Functional Theory 10

2.3.1 The Electron Density 11

2.3.2 Hohenberg-Kohn Theorems 12

2.3.3 Advantage and Disadvantage of Hohenberg-Kohn Theorems . 14

2.3.4 Kohn-Sham Equation: Reformulating Many-Body Problems . 15

2.3.5 The Role and Calculation of Exchange-Correlation 18

3 Results and Discussion **20**

3.1 Computational Details 20

3.2 Structural properties 21

3.3 Electronic properties . . . 22
3.3.1 Band structures . . . 22
3.3.2 Density of states . . . 23
3.4 Electron density . . . 25
3.5 Optical properties . . . 26
3.5.1 Dielectric function . . . 26
3.5.2 Absorption coefficient . . . 28
3.5.3 Optical conductivity . . . 28
3.5.4 Reflectivity . . . 29
3.5.5 Refractive index . . . 30
3.6 Thermoelectric characteristics . . . 30

4 Conclusion **33**

Bibliography **34**

List of Figures

2.1 Flowchart illustrating the iterative process for solving the Kohn-Sham equation in density functional theory to obtain the ground-state electron density and associated properties of a many-body system. 18

3.1 The Crystallographic structure of RbSrBi. 21

3.2 Energy vs volume optimization curve of RbSrBi. 22

3.3 Band Structure of RbSrBi for (a) PBE-GGA and for (b) TB-mBJ potential. 23

3.4 (a) Total density of states (TDOS) of RbSrBi and partial density of states (PDOS) of (b) Rb (c) Sr and (d) Bi atoms. 24

3.5 Electron density of RbSrBi for (100) and (110) plane. 25

3.6 (a) Real dielectric function and (b) Imaginary dielectric function of RbSrBi. 27

3.7 (a) Absorption coefficient (b) Optical conductivity of RbSrBi of RbSrBi. 28

3.8 (a) Optical Reflectivity and (b) Refractive index of RbSrBi. 29

3.9 (a) Electrical Conductivity (b) Electronic Thermal Conductivity of RbSrBi. 31

3.10 (a) Seebeck coefficient (b) Power factor and (c) Figure of merit and of RbSrBi. 32

Investigation on optoelectronic and thermoelectric characteristics of half-Heusler compound RbSrBi: A first-principles study

Chapter 1

Introduction

As global energy demand rises and natural resources are depleted, there is an urgent need for alternative energy solutions. One promising option is the development of thermoelectric materials that can convert waste heat into usable energy. This technology is gaining attention in sustainable energy research, especially for its potential in harnessing solar power [1–3]. Thermoelectric power generation offers a practical solution to the world's energy challenges. It can generate power from waste heat while also helping conserve energy. These materials can be powered by various heat sources, such as combustion, sunlight, chemical reactions, and nuclear decay, making them a flexible and efficient way to produce energy [4–6]. The dimensionless figure of merit (ZT), which may be written as ZT = $(\sigma S^2/\kappa)$, is commonly used to assess the performance of thermoelectric devices. The power factor (PF) is denoted by the formula σS^2, where S stands for the Seebeck coefficient, σ for electrical conductivity, T for absolute temperature, and κ for thermal conductivity [7–9]. Optimizing power factor while reducing thermal conductivity is necessary to achieve good performance in thermoelectric materials [10, 11]. As a result, various theoretical investigations and tests focused on its thermoelectric characteristics. The optical and thermoelectric characteristics of the nonmagnetic half-Heuslers (HHs) have been studied by various groups [12, 13]. Researchers have been studying several half-Heuslers

compounds because of these remarkable characteristics, primarily those with the face-centered cubic structure, which is a member of the $F\bar{4}3m$ space group [14–16].

Several half-Heuslers that can be used in solar cells and are appropriate for optoelectronic devices were studied by Gruhn et al. [17]. Kacimi et al. [18] studied a variety of HHs of I-II-V and I-III-IV, exposing their structural, optoelectronic and thermoelectric characteristics. The thermoelectric characteristics of KScY (Y = C, Ge) that show notable transport qualities that are significantly superior than the initial material, Bi_2Te_3, have been reported by Yasemin et al. [19] in their investigations. According to Deepika et al., the KScX (X = Sn, Pb) and KYX (X = Si, Ge) HHs have excellent power factors and are suitable for thermoelectric applications [20, 21]. The above-mentioned results inspired us to learn more about half-Heusler compounds. Recent research on a variety of half-Heusler alloys' structural, optoelectronic, thermoelectric, mechanical, magneto-electronic, low thermal conductivity, and spin-orbit coupling effects has been published in the literature [22–27].

We follow the first-principle calculation method using Density Functional Theory (DFT) as implemented in the WIEN2k code. The electronic structure of atoms, molecules and solids is studied using a computational technique called density functional theory (DFT), in quantum mechanics. It simplifies calculations by focusing on electron density rather than directly solving complex equations, making it a valuable tool for predicting material properties, simulating chemical reactions, and advancing research in materials science and nanotechnology [28]. Peter Blaha and his team created the potent software program WIEN2k, which applies the Full Potential Linearized Augmented Plane Wave (FP-LAPW) technique [29]. WIEN2k is well known for its precision and may be used to analyze a wide range of materials, including metals, insulators, and magnetic materials. It plays a crucial role in investigating electronic and magnetic properties, predicting crystal structures, and unraveling complex phenomena in condensed matter physics and materials science.

The structural, optoelectronic, and thermoelectric properties of the RbSrBi half-Heusler compound is investigated here by first-principles simulations. To the best of our knowledge, no thorough investigation has been conducted on this material

yet. An exact computation of the electrical band structure is required in order to reproduce believable results of related properties. Since the Tran-Blaha modified Becke-Johnson (TB-mBJ) exchange potential has been shown to accurately predict the band gap of solids, it is used in this investigation. According to the results, the RbSrBi half-Heusler compound under investigation may be a great option for thermoelectric generators and other optical devices. We anticipate that the current study's findings will be helpful for future theoretical and experimental research on other half-Heuslers.

The arrangements of this project are such that an introduction is given in Chapter 1. In chapter 2, we discuss about the theoretical background including the basic quantum mechanics as the basis of density functional theory. Starting from Schrödinger equation, we briefly discuss the Born-Oppenheimer approximation and the Hartee-Fock approximation with its limitations and the theoretical density functional theory in this chapter. In chapter 3, we discuss the structural, electronic, optical and thermoelectric properties of RbSrBi. In last chapter, we summarize our findings on the characteristics and potential applications of the materials.

Chapter 2

Theoretical background

Density Functional Theory (DFT) is one of the most widely used computational methods in quantum mechanics, providing a powerful framework for studying the electronic structure of matter. By modeling the behavior of electrons within atoms, molecules, and solids, DFT has become an essential tool in fields such as chemistry, physics, and materials science. Unlike traditional wave-function-based methods, DFT simplifies the complex many-body problem by focusing on electron density as the fundamental quantity, rather than dealing directly with the more complicated wave functions. This shift allows DFT to efficiently describe systems with many particles while maintaining a high level of accuracy. The development of DFT was spearheaded by Walter Kohn, who was awarded the Nobel Prize in Chemistry in 1998 for his pioneering work [30]. Kohn's contributions revolutionized the way scientists solve the Schrödinger equation for multi-electron systems. Today, DFT strikes a balance between computational cost and precision, making it suitable for large-scale simulations in both research and industrial applications. It is indispensable for investigating a wide range of properties, from chemical reactivity and molecular dynamics to the electronic, mechanical, and optical behavior of materials, helping to unlock new insights into the fundamental nature of matter [31]. This chapter provides an overview of fundamental quantum mechanics, the challenges it presents,

and how Density Functional Theory (DFT) addresses these challenges to enable efficient analysis of complex systems.

2.1 Basic Quantum Mechanics

To understand the foundation of Density Functional Theory (DFT), it is essential to first revisit the fundamental principles of quantum mechanics. Quantum mechanics provides the framework for describing the behavior of particles at the atomic and subatomic levels. Central to this framework is the Schrödinger equation, which governs the dynamics of quantum systems and allows us to derive important properties such as energy levels and wave unctions [32]. The Schrödinger equation can be expressed in both time-dependent and time-independent forms. We will focus on the time-independent Schrödinger equation, which is particularly relevant for stationary states of quantum systems. The solutions to this equation give wave functions, which describe the likelihood of where particles are and how they move, as well as the energy eigenvalues, which represent the possible energy levels of the system. Together, these help us understand how electrons behave in atoms and molecules. [33]

2.1.1 Schrödinger Equation

The Schrödinger equation is a fundamental equation in quantum mechanics that describes the quantum state of a physical system. It is crucial for understanding the behavior of particles at the atomic and subatomic levels, such as electrons, photons, and other quantum objects. First formulated by Erwin Schrödinger in 1925, this equation provides a mathematical framework for predicting the properties and behavior of quantum systems. [34] The mathematical form of the Schrödinger equation is

$$\hat{H}\psi = E\psi \tag{2.1}$$

where, $\hat{H}$ is the Hamiltonian operator, ψ is the wave function of the system, and E is the energy eigenvalue corresponding to the quantum state described by ψ.

This equation is crucial in finding the stationary states of quantum systems. The Hamiltonian, $\hat{H}$, represents the total energy operator of the system and is typically composed of two parts: the kinetic energy operator, $\hat{T} = -\frac{\hbar^2}{2m}\nabla^2$ and the potential energy operator, $\hat{V} = \mathrm{V}\ (\mathbf{r})$. The kinetic energy operator describes the motion of particles, while the potential energy operator accounts for the forces acting on them due to their positions within the system. Together, these components determine the total energy of the quantum system. Hence, the Schrödinger equation in three dimensions becomes

$$[-\frac{\hbar^2}{2m}\nabla^2 + V(\mathbf{r})]\psi(\mathbf{r}) = E\psi(\mathbf{r}). \tag{2.2}$$

2.1.2 Wave Functions and Probability Density

The wave function, $\psi(\mathbf{r})$, is a fundamental concept in quantum mechanics. It encapsulates all the information about the quantum state of a system, including the likelihood of finding particles in particular positions $\mathbf{r}$ and with specific properties. In essence, ψ encodes the physical behavior of the system and allows us to calculate observable quantities, such as energy, by solving the Schrödinger equation. The wave function is generally a complex function that depends on the position of particles in the system. While ψ itself does not have direct physical meaning, it is crucial for calculating observable properties of particles. The square of the wave function, $|\psi|^2$, represents the probability distribution for the positions of particles, offering critical insights into their behavior within the quantum system.

2.2 The Many-Body Problem

The many-body problem in quantum mechanics addresses the challenge of describing systems comprising multiple interacting atoms. Unlike single-atom systems, which can often be analyzed using analytical solutions, many-body systems involve intricate interactions that lead to emergent phenomena, such as correlations and collective behaviors. The Hamiltonian of a many-body system consisting of nuclei

and electrons can be written as,

$$\hat{H} = \hat{T}_{nuclei} + \hat{T}_{electrons} + \hat{V}_{nn} + \hat{V}_{ee} + \hat{V}_{ne} \tag{2.3}$$

with the terms representing:

- $\hat{T}_{nuclei}$: the kinetic energy of the nuclei,
- $\hat{T}_{electrons}$: the kinetic energy of the electrons,
- $\hat{V}_{nn}$: the nucleus-nucleus Coulomb repulsion,
- $\hat{V}_{ee}$: the electron-electron Coulomb repulsion,
- $\hat{V}_{ne}$: the attractive interaction between nuclei and electrons.

These interaction terms make solving the Schrödinger equation for large systems of atoms exceedingly complex. The Coulomb interactions $\hat{V}_{nn}$, $\hat{V}_{ee}$ and $\hat{V}_{ne}$ describe the forces between particles, which must be accounted for when determining the total energy of the system. As the number of atoms increases, the number of interactions grows rapidly, making direct analytical or numerical solutions impractical. With the explicit forms of the kinetic energies and interaction terms, the many-body Hamiltonian for a system consisting of nuclei and electrons becomes:

$$\hat{H} = \hat{T}_{nuclei} + \hat{T}_{electrons} + \hat{V}_{nn} + \hat{V}_{ee} + \hat{V}_{ne}$$

$$\hat{H} = -\sum_{I} \frac{\hbar^2}{2m_I} \nabla^2_{\mathbf{R}_I} - \sum_{i} \frac{\hbar^2}{2m_e} \nabla^2_{\mathbf{r}_i} + \frac{1}{2} \sum_{I,J} \frac{Z_I Z_J e^2}{|\mathbf{R}_I - \mathbf{R}_J|} + \frac{1}{2} \sum_{i,j} \frac{e^2}{|\mathbf{r}_i - \mathbf{r}_j|} - \sum_{I,i} \frac{Z_I e^2}{|\mathbf{R}_I - \mathbf{r}_i|}. \tag{2.4}$$

Here, the indices I and J run over the nuclei, while i and j run over the electrons. R_I and M_I are the position and mass of the nuclei, respectively, and $\mathbf{r}_i$ and m_e are the position and mass of the electrons. The terms $|\mathbf{R}_I - \mathbf{R}_J|$, $|\mathbf{R}_I - \mathbf{r}_i|$, and $|\mathbf{r}_i - \mathbf{r}_j|$ represent the distances between nuclei-nuclei, nuclei-electrons, and electrons-electrons, respectively. Z_I is the atomic number of the I-th nucleus.

Solving the many-body Hamiltonian presents several significant challenges in quan-

tum mechanics, particularly in systems involving both electrons and nuclei. The high dimensionality of the problem is a major hurdle; for a system with N electron and M nuclei, the wave function depends on $3(N + M)$ variables, making analytical solutions increasingly intractable as N and M increase. Additionally, the Coulomb interactions between electrons introduce complex correlations, complicating the treatment of each electron as an independent particle. Furthermore, since electrons are fermions, they must adhere to the Pauli exclusion principle, requiring that the many-body wave function is antisymmetric under the exchange of particles, which adds another layer of complexity. The potential energy terms in the Hamiltonian, which encompass nucleus-nucleus and nucleus-electron interactions, further contribute to the difficulty. While analytical solutions are only feasible for very simple systems, such as the hydrogen atom, most many-body systems with multiple electrons and nuclei do not permit exact solutions.

2.2.1 Born-Oppenheimer Approximation

Given the complexities associated with the many-body Hamiltonian, particularly in systems containing both electrons and nuclei, it becomes essential to simplify the problem for practical analysis. One of the most widely used approaches is the Born-Oppenheimer approximation, which exploits the significant difference in mass and, consequently, the motion between electrons and nuclei. Since nuclei are much more massive than electrons, their motion can be considered relatively slow compared to the fast-moving electrons. This allows us to treat the nuclei as fixed in space while solving for the electronic wave functions. By separating the total wave function into electronic and nuclear components, the Born-Oppenheimer approximation reduces the complexity of the many-body Schrödinger equation.

Under this approximation, the total Hamiltonian can be expressed as a sum of two parts: the electronic Hamiltonian $\hat{H}_{el}$, which describes the motion of electrons in the field of fixed nuclei, and the nuclear Hamiltonian $\hat{H}_{nuc}$, which accounts for the motion of the nuclei interacting with each other. The total Hamiltonian $\hat{\mathrm{H}}$ is then

given by:

$$\hat{H} = \hat{H}_{el} + \hat{H}_{nuc} \tag{2.5}$$

where

$$\hat{H}_{el} = -\sum_{i} \frac{\hbar^2}{2m_e} \nabla_{ri}^2 + \frac{1}{2} \sum_{i,j} \frac{e^2}{|r_i - r_j|} - \sum_{I,i} \frac{Z_I e^2}{|R_I - r_i|} \tag{2.6}$$

and

$$\hat{H}_{nuc} = \sum_{I} \frac{\hbar^2}{2m_I} \nabla_{RI}^2 + \frac{1}{2} \sum_{I,J} \frac{Z_I Z_J e^2}{|R_I - R_J|}. \tag{2.7}$$

This simplification allows for easier calculations since the focus is primarily on the electronic structure. In many cases, especially in density functional theory, the nuclei are often treated as fixed due to their relatively large mass compared to electrons. This approximation streamlines the calculations by reducing the complexity of the system to that of the electrons interacting in a static potential created by the fixed nuclei. However, if nuclear motion needs to be included, the Schrödinger equation for the nuclei can be solved, treating them as quantum mechanical entities. The total energy E_{total} of the system is then obtained as the sum of the electronic energy and the nuclear energy.

Once the electronic Hamiltonian $\hat{H}_{el}$ is defined, the electronic Schrödinger equation can be expressed as:

$$\hat{H}_{el}\psi(\mathbf{r}1, \mathbf{r}2, ..., \mathbf{r}N) = E\psi(\mathbf{r}_1, \mathbf{r}_2, ..., \mathbf{r}_N). \tag{2.8}$$

In this equation, $\Psi(\mathbf{r}_1, \mathbf{r}_2, ..., \mathbf{r}_N)$ is the many-body wave function, which depends on the positions of all N electrons, and E represents the total energy of the system. Solving this many-body electronic Schrödinger equation poses several challenges. The wave function Ψ is a complex function of all electron coordinates, making it difficult to handle analytically, especially as N increases. Additionally, capturing the correlation between electrons, particularly in systems with strong electron-electron interactions, adds to the complexity. Using all approximations introduced up to now, it is possible to calculate a problem similar to H_2^+, a single ionized hydrogen molecule. To get results for larger systems, further approximations have to be made.

2.2.2 Hartree-Fock Approximation and Its Limitations

The Hartree-Fock (HF) approximation is a fundamental method in quantum chemistry used to approximate the many-body wave function of a system of electrons. It represents the wave function as a Slater determinant, ensuring the antisymmetry required by the Pauli exclusion principle. This determinant combines single-electron wave functions (orbitals) into a single function that changes sign upon the exchange of two electrons.

However, the Hartree-Fock method has notable limitations. It employs a mean-field approximation, where each electron moves in an average field created by all others. This approach neglects electron correlation effects, which are essential for accurately describing many-electron systems, especially those with strong correlations. Consequently, Hartree-Fock often yields inaccurate results for properties such as bond lengths, reaction energies, and excitation energies.

Moreover, while the Slater determinant accounts for antisymmetry, it fails to capture dynamic electron correlation arising from instantaneous electron-electron interactions. Another drawback is its computational cost, which scales as $O(N^4)$, where N is the number of electrons. This steep scaling results from the need to evaluate numerous orbital integrals, making HF computationally expensive for large systems. Despite these limitations, Hartree-Fock remains a foundational approach, forming the basis for more advanced post-Hartree-Fock HF methods.

2.3 Density Functional Theory

Density Functional Theory (DFT) is a powerful quantum mechanical modeling method widely used to investigate the electronic structure of many-body systems. Unlike traditional methods that rely on wave functions, DFT is based on the electron density, which is considered a fundamental variable. The key idea behind DFT is that all properties of a system can be determined from its electron density rather than the many body wave function. This approach simplifies the problem of solving the Schrödinger equation, as it reduces the complexity associated with many-body

interactions. DFT is particularly advantageous because it balances accuracy and computational efficiency, allowing researchers to study larger and more complex systems than would be feasible with wave-function-based methods. By leveraging the Hohenberg-Kohn theorems and the Kohn-Sham equations, DFT provides a practical framework for exploring a wide range of physical, chemical, and material properties [35].

2.3.1 The Electron Density

In Density Functional Theory (DFT), the electron density n($\mathbf{r}$) serves as the central variable for describing a quantum system. The electron density represents the probability of finding an electron at a particular point in space and can be derived from the many-body wave function $\psi(r_1, r_2, ..., r_N)$ by integrating over all electron coordinates. This relationship is expressed mathematically as: [36, 37]

$$n(\mathbf{r}) = N \int |\psi(\mathbf{r}_1, \mathbf{r}_2, ..., \mathbf{r}_N)|^2 d\mathbf{r}_2 d\mathbf{r}_3 ... d\mathbf{r}_N. \tag{2.9}$$

Additionally, we must remember that all electrons are identical; thus, we cannot label them as electron 1 or electron N . Instead, we can determine the probability of any order or set of N electrons being located at the coordinates $\mathbf{r}_1$ to $\mathbf{r}_N$. While the wave function contains comprehensive information about the quantum state of a system, it is the electron density that ultimately determines all measurable properties. The total number of electrons N in the system can also be calculated from the electron density using the equation:

$$N = \int n(\mathbf{r}) d\mathbf{r} \tag{2.10}$$

This integration highlights that the electron density encodes vital information about the total number of electrons, making it a fundamental aspect of DFT. By focusing on n($\mathbf{r}$) instead of the complex multi-dimensional wave function, DFT simplifies calculations, making it a practical and efficient approach for studying the electronic structure of various materials.

2.3.2 Hohenberg-Kohn Theorems

Density functional theory as we know it today was born in 1964 when a landmark paper by Hohenberg and Kohn appeared in the *Physical Review* [37]. The theorems they introduced represent the major theoretical pillars on which all modern-day density functional theories are built. These theorems laid the groundwork for the fundamental relationship between electron density and the properties of quantum systems, making DFT a powerful alternative to wave-function-based methods. The Hohenberg-Kohn theorems are central to the formulation of DFT, and they can be summarized as follows:

First theorem: The ground-state electron density n($\mathbf{r}$) uniquely determines the external potential $V_{ext}(\mathbf{r})$ acting on the electrons. This means that if the electron density of a system is known, the external potential can be uniquely inferred, allowing for the derivation of all ground-state properties, including the total energy, from the electron density.

According to the first theorem, the ground-state density and the external potential correspond in a one-to-one manner. Since the external potential is fixed, the Hamiltonian, and hence the wave function Ψ, is determined by the ground-state density $n_0(\mathbf{r})$. The proof of this theorem is straightforward: Consider the ground states of two N-electron systems, characterized by two different external potentials $V_{ext}(\mathbf{r})$ and $V'_{ext}(\mathbf{r})$, which differ by more than an additive constant. The corresponding Hamiltonians, $\hat{H}$ and $\hat{H}'$, would both have the same ground-state density n($\mathbf{r}$), but different ground-state wave functions, Ψ and Ψ', with $\hat{H}\Psi = E_0\Psi$ and $\hat{H}'\Psi' = E'_0\Psi'$. Since Ψ' is not the ground state of $\hat{H}$, it follows that

$$\begin{aligned} E_0 &< \langle \Psi' | \hat{H} | \Psi' \rangle \\ &< \langle \Psi' | \hat{H}' | \Psi' \rangle + \langle \Psi' | \hat{H} - \hat{H}' | \Psi' \rangle \\ &< E'_0 + \int n_0(\mathbf{r}) V_{\text{ext}}(\mathbf{r})\, d\mathbf{r} \end{aligned} \tag{2.11}$$

Similarly,

$$\begin{aligned} E_0' &< \langle\Psi|\hat{H}'|\Psi\rangle \\ &< \langle\Psi|\hat{H}|\Psi\rangle + \langle\Psi|\hat{H}' - \hat{H}|\Psi\rangle \\ &< E_0 + \int n_0(\mathbf{r})\big[V_{\text{ext}}'(\mathbf{r}) - V_{\text{ext}}(\mathbf{r})\big]\, d\mathbf{r}. \end{aligned} \tag{2.12}$$

Adding equation (11) and equation (12) leads to the contradiction,

$$E_0 + E_0' < E_0 + E_0' \tag{2.13}$$

Hence, no two different external potentials $V_{ext}(\mathbf{r})$ can give rise to the same ground state density $n_0(\mathbf{r})$ which determines the external potential $V_{ext}(\mathbf{r})$, except for a constant. That is to say, there is a one-to-one mapping between the ground state density $n_0(\mathbf{r})$ and the external potential $V_{ext}(\mathbf{r})$, although the exact formula is unknown.

Second theorem: For any trial electron density n($\mathbf{r}$), the energy functional E[n] will yield a value that is greater than or equal to the ground-state energy E_0. The equality holds when the trial density corresponds to the true ground-state density. This variational principle implies that one can minimize the energy functional E[n] with respect to the electron density to find the ground state of a system.

There exists a universal functional F[n($\mathbf{r}$)] of the density, independent of the external potential $V_{ext}(\mathbf{r})$, such that the minimum value of the energy functional

$$E[n(r)] \equiv \int n(r)V_{ext}(\mathbf{r})dr + F[n(\mathbf{r})] \tag{2.14}$$

yields the exact ground-state energy of the system. The exact ground-state density $n_0(\mathbf{r})$ minimizes this functional. Thus, the exact ground-state energy and density are fully determined by the functional E[n($\mathbf{r}$)]. The universal functional F[n($\mathbf{r}$)] can be written as:

$$F[n(r)] \equiv T[n(\mathbf{r})]r + E_{int}[n(\mathbf{r})] \tag{2.15}$$

where T [n($\mathbf{r}$)] is the kinetic energy and $E_{int}[n(\mathbf{r})]$ is the interaction energy of the particles. According to the variational principle, for any wave function Ψ', the energy

functional

$$E[\Psi'] \equiv <\Psi'|\hat{T} + \hat{V}_{int} + \hat{V}_{ext}|\Psi'> \tag{2.16}$$

reaches its global minimum only when Ψ' is the ground-state wave function Ψ_0, with the constraint that the total number of particles is conserved. According to the first Hohenberg-Kohn theorem, Ψ' must correspond to a ground state with particle density $n'(\mathbf{r})$, making $E\Psi'$ a functional of $n'(\mathbf{r})$. Applying the variational principle:

$$E[\Psi'] = \int n'(\mathbf{r})V_{ext}(\mathbf{r})dr + F[n'(\mathbf{r})] > E[\Psi_0] = \int n_0(\mathbf{r})V_{ext}(\mathbf{r})dr + F[n_0(\mathbf{r})] = E[n_0(\mathbf{r})] \tag{2.17}$$

Thus, the energy functional $E[\Psi] \equiv \int n(\mathbf{r})V_{ext}(\mathbf{r})dr + F[n(\mathbf{r})]$ evaluated for the correct ground-state density $n_0(r)$ is lower than the value of this functional for any other density n($\mathbf{r}$). Therefore, by minimizing the total energy functional of the system with respect to variations in the density n($\mathbf{r}$), one can find the exact ground-state density and energy. This functional, however, only determines ground-state properties and does not provide any insight into excited states.

2.3.3 Advantage and Disadvantage of Hohenberg-Kohn Theorems

The Hohenberg-Kohn theorems are fundamental to density functional theory and offer significant advantages in computational chemistry and materials science. One of the primary benefits is their ability to relate the ground-state properties of many-electron systems directly to electron density, simplifying calculations compared to wave-function-based methods. The first theorem establishes a unique mapping between the ground-state electron density and the external potential, ensuring that all ground-state properties can be derived from the electron density alone. Additionally, the second theorem introduces a variational principle that allows for the efficient optimization of electron density to find the ground state. By shifting the focus from finding a function of $3N$ variables (the wave function) to a function of three variables (the electron density), the Hohenberg-Kohn theorems significantly simplify the process of resolving the Schrödinger equation. These theorems make

DFT a versatile tool applicable to a wide range of systems, from small molecules to large biological complexes.

However, the Hohenberg-Kohn theorems also come with notable disadvantages. They are limited to ground-state properties, providing no direct insight into excited states, which poses challenges in studying electronic excitations and charge transfer processes. The effectiveness of DFT is highly dependent on the choice of exchange-correlation func- tional, which may not accurately capture all correlation effects, especially in systems with strong electron-electron interactions. Furthermore, while DFT is generally computationally less intensive than wave-function methods, the calculations of exchange-correlation energies can still be demanding. The reliance on external potentials and the interpretation challenges associated with electron density further highlight the limitations of the Hohenberg-Kohn theorems, necessitating careful consideration when applying DFT to complex systems.

2.3.4 Kohn-Sham Equation: Reformulating Many-Body Problems

The Kohn-Sham equation is a central component of density functional theory that allows for the practical calculation of electronic structures in many-body systems. It stems from the foundational Hohenberg-Kohn theorems, which established the uniqueness of the ground-state electron density and its relationship with the external potential. The Kohn- Sham framework reformulates the complex many-body problem into a set of simpler, non-interacting single-particle equations, making it more tractable for computational purposes.

In the Kohn-Sham approach, the true interacting electron system is mapped onto an auxiliary system of non-interacting electrons that yield the same electron density as the original system. This is achieved through the Kohn-Sham equations [38], which can be expressed as:

$$(-\frac{\hbar^2}{2m_e}\nabla^2 + V_{eff})\psi_i(\mathbf{r}) = \epsilon_i\psi_i(\mathbf{r}), \tag{2.18}$$

where $V_{eff}(\mathbf{r})$ is the effective potential that includes the external potential and the

exchange- correlation potential. The Kohn-Sham orbitals $\psi_i(\mathbf{r})$ are used to construct the electron density n($\mathbf{r}$) as:

$$n(r) = \sum_i |\psi_i(r)|^2. \tag{2.19}$$

This approach significantly reduces the complexity of solving the many-body Schrödinger equation by allowing for the treatment of a system of independent particles, while still capturing the essential effects of electron correlation through the exchange-correlation functional.

The effective potential in the Kohn-Sham framework can be expressed as:

$$V_{eff} = V_{ext} + V_{Hartree}[n(\mathbf{r})] + V_{xc}[n(\mathbf{r})]. \tag{2.20}$$

Here, V_{ext} represents the external potential acting on the electrons in the system. This potential typically arises from the interaction between the electrons and fixed nuclei or any other external fields applied to the system. In many cases, V_{ext} is described by the Coulomb potential due to the nuclei, reflecting how electrons experience attraction towards positively charged atomic cores. This term plays a crucial role in determining the overall potential landscape in which the electrons move, significantly influencing the electronic structure of the system.

The term $V_{Hartree}[n(\mathbf{r})]$ is the Hartree potential, which describes the classical electrostatic interaction between electrons in a many-body system. It accounts for the repulsion between charged particles, reflecting that the potential energy experienced by an electron is due to the distribution of other electrons around it. The Hartree potential is calculated as:

$$V_{Hartree}[n(\mathbf{r})] = e^2 \int \frac{n(\mathbf{r}')}{|r - \mathbf{r}'|} d\mathbf{r} \tag{2.21}$$

This formulation integrates the electron density n($\mathbf{r}$) over all space, considering the effect of all other electrons on a given electron located at $\mathbf{r}$. This approach provides a mean-field treatment of electron-electron repulsion, avoiding the complexity of

considering every pair of interactions explicitly.

The exchange-correlation potential $V_xc[n(\mathbf{r})]$ represents the quantum mechanical effects of exchange and correlation among electrons. It is defined as:

$$V_{xc}[n(\mathbf{r})] = \frac{\delta E_{xc}[n]}{\delta n} \tag{2.22}$$

The exchange term arises from the antisymmetry requirement of the total wave function for fermions, accounting for the reduction in energy when two electrons are spatially separated. The correlation term reflects the correlated motion of electrons that cannot be captured by a mean-field approach, accounting for the ways in which the presence of one electron affects the probability distribution of another electron's position and momentum. From these considerations, the Kohn-Sham Hamiltonian can be formulated as:

$$\hat{H}_{KS} = -\frac{\hbar^2}{2m_e}\nabla^2 + V_{ext} + V_{Hartree}[n(\mathbf{r})] + V_{xc}[n(\mathbf{r})]. \tag{2.23}$$

The major distinction between the Kohn-Sham formulation and the Hartree formulation lies in the inclusion of both exchange and correlation effects in the effective potential, providing a more accurate description of many-body systems.

Solving the Kohn-Sham equation is a crucial step in density functional theory for obtaining the ground-state electron density of a many-body system. In a condensed matter system, the Kohn-Sham equation provides a method to derive the exact density and energy of the ground state. The process begins with an initial electron density n($\mathbf{r}$), typically a superposition of atomic electron densities. The effective Kohn-Sham potential V_{eff} is then calculated, and the Kohn-Sham equation is solved to obtain single-particle eigenvalues and wave functions. A new electron density is subsequently calculated from these wave functions.

This iterative process is commonly performed numerically through self-consistent iterations, as illustrated in the flowchart figure 2.1. The self-consistency can be determined by monitoring the change in total energy, electron density from the previous iteration, or the total force acting on the atoms being less than a specified

small quantity, or by using a combination of these criteria. If self-consistency is not achieved, the calculated electron density is mixed with the density from previous iterations to derive a new electron density, and the process repeats. This continues until self-consistency is reached [39]. Once convergence is achieved, various quantities can be calculated, including total energy, forces, stress, eigenvalues, electron density of states, and band structure, among others.

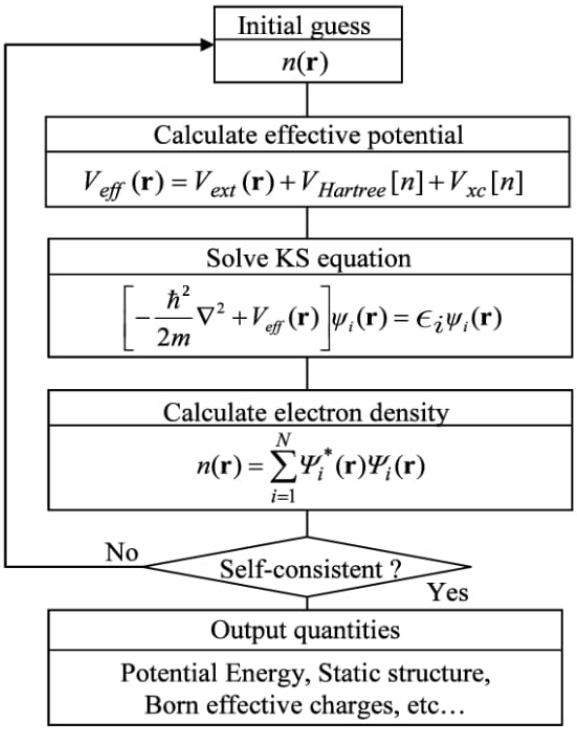


Figure 2.1: Flowchart illustrating the iterative process for solving the Kohn-Sham equation in density functional theory to obtain the ground-state electron density and associated properties of a many-body system.

2.3.5 The Role and Calculation of Exchange-Correlation

In density functional theory, the exchange-correlation potential, $V_{xc}[n(\mathbf{r})]$, is a critical component that captures the complex quantum mechanical effects of electron exchange and correlation. However, V_{xc} is not derived exactly but is instead approximated due to the computational challenges of dealing with many-electron systems. One of the most common approximations is the Local Density Approximation (LDA), where V_{xc} is considered to depend solely on the local electron density. This

approximation is based on the idea that in regions where the electron density is nearly uniform, the behavior of electrons can be likened to that of a homogeneous electron gas. While simple, LDA can perform reasonably well for certain materials, especially solids with nearly uniform electron densities.

To improve upon the LDA, the Generalized Gradient Approximation (GGA) introduces a dependence on the spatial gradients of the electron density. By including information about how the density changes in space, GGA provides more accurate results for systems where the density varies significantly, such as in molecules or surfaces. These improvements make GGA one of the most widely used approximations in modern DFT calculations. More advanced methods, such as hybrid functionals, combine the exchange from exact Hartree-Fock theory with the approximate exchange-correlation from LDA or GGA. Hybrid functionals, like B3LYP, tend to improve accuracy further, particularly for molecular systems, by including a portion of exact exchange, which LDA and GGA inherently miss [40].

In practice, the calculation of V_{xc} is an iterative process within the self-consistent field (SCF) method. The DFT algorithm begins with an initial guess for the electron density, usually based on atomic configurations. Using this initial density, the Kohn-Sham equations are solved to update the potential and electron density. The exchange-correlation potential, V_{xc}, is recalculated at each step based on the updated density. This process continues until the electron density converges to a self-consistent solution, meaning that the input and output densities agree within a set tolerance. Recent developments also include meta-GGA functionals, which incorporate even higher-order density-related terms, such as the kinetic energy density, to account for more complex interactions. While computationally more expensive, these functionals can offer improved accuracy for systems with intricate electronic structures. Thus, although V_{xc} is not known exactly, various approximations—from LDA and GGA to hybrid and meta-GGA functionals—allow DFT to achieve a good balance between accuracy and computational efficiency for a wide range of materials and molecular systems.

Chapter 3

Results and Discussion

The investigation of structural, optoelectronic, and thermoelectric characteristics are described in this chapter. To explain these findings properly, it is necessary to understand the computational techniques. We will describe with the computational methodologies in the next section.

3.1 Computational Details

The structural, electronic, optical and thermoelectric properties of the investigated materials were studied using Density Functional Theory (DFT) within the Full Potential Linearized Augmented Plane Wave (FP-LAPW) framework [41–43]. The WIEN2k code was employed for all computational analyses [44]. Structural optimizations were performed using the Murnaghan equation of state to determine equilibrium lattice parameters. For the volume optimization, using the Generalized Gradient Approximation (GGA) as formulated by Perdew, Burke and Ernzerhof (PBE) was used as the exchange-correlation functional [40]. To accurately evaluate the electronic properties and address the common underestimation of band gap values associated with the PBE-GGA approach, the Tran-Blaha modified Becke-Johnson (TB-mBJ) potential was applied [45]. The energy convergence and charge

convergence were set to 0.00001 Ry and 0.0001 e respectively, where e is the electron charge. We set to RK_{max}=7 for wavefunction expansions, where R is the smallest muffin-tin radius and K_{max} is the largest reciprocal lattice vector used in the expansion of the plane wave functions. The largest expansion Fourier of charge density was up to G_{max}=12 (a.u.)$^{-1}$, and angular momentum vector l_{max}=10. The Brillouin zone was sampled using a dense k-mesh of 3000 points to ensure high accuracy. Optical properties were analyzed using the Kramers-Kronig relations, while thermoelectric properties were investigated using the Boltzmann transport theory as implemented in the BoltzTraP code [46]. This comprehensive approach provided reliable insights into the structural, electronic, optical, and thermoelectric behavior of the materials.

3.2 Structural properties

This section explores the structural characteristics of the compound RbSrBi. Investigating the microscopic structure of materials is particularly valuable, as it significantly impacts the prediction of other properties, such as electrical and thermal behavior. Notably, the half-Heusler compounds exhibit a non-centrosymmetric cubic structure with a space group of $F\bar{4}3m$(#216), as illustrated in figure 3.1. In

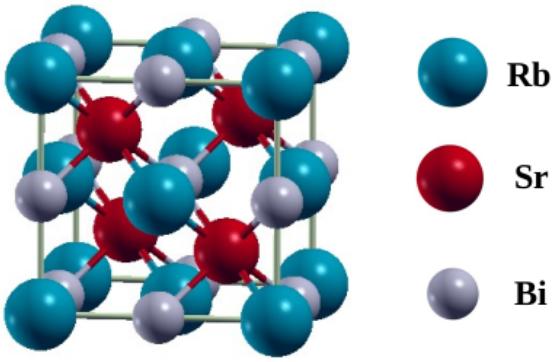


Figure 3.1: The Crystallographic structure of RbSrBi.

the RbSrBi compound, the atomic positions are defined as follows: the Rb atom is located at (0, 0, 0), the Sr atom at (0.25, 0.25, 0.25), and the Bi atom at (0.0, 0.0, 0.5). The lattice constant for RbSrBi has been determined to be 8.12 Å [47]. However, due to the lack of prior studies on this compound, no comparative analysis

is available.

To determine the most stable structure with the system's ground state energy, a volume optimization computation has been carried out. The structural properties of the RbSrBi half-Heusler compound were analyzed using the Murnaghan equation of state [48]. Figure 3.2 illustrates the energy versus volume optimization curve.

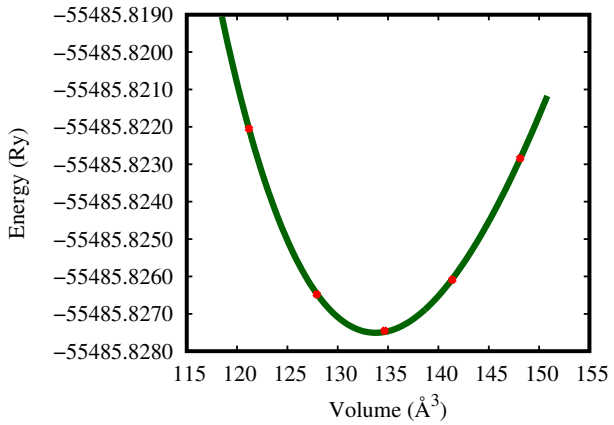


Figure 3.2: Energy vs volume optimization curve of RbSrBi.

The calculated minimum energy and corresponding volume are -55485.8274 Ry and 133.85 $Å^3$ respectively, also shown in figure 3.2. We determined the optimized lattice constant for the primitive unit cell, generated the crystallographic structure and evaluated the total energy for the conventional unit cell.

3.3 Electronic properties

3.3.1 Band structures

The configuration of energy levels, or bands, occupied by electrons in a material is called band structure. Band structure is crucial for understanding a material is conductor, semiconductor or insulator. The electronic band structures of RbSrBi compounds were analyzed to evaluate their potential for electronic applications. Figure 3.3 presents the predicted band structures obtained using various computational approaches. Both the valence band maximum and the conduction band minimum are located at the gamma-point, indicating that the studied half-Heusler compounds

exhibit a direct bandgap. Specifically, for RbSrBi, the calculated bandgap value using the PBE-GGA method is determined to be 0.849 eV. Using the TB-mBJ approximation, the bandgap value of RbSrBi is predicted to be 1.583 eV.

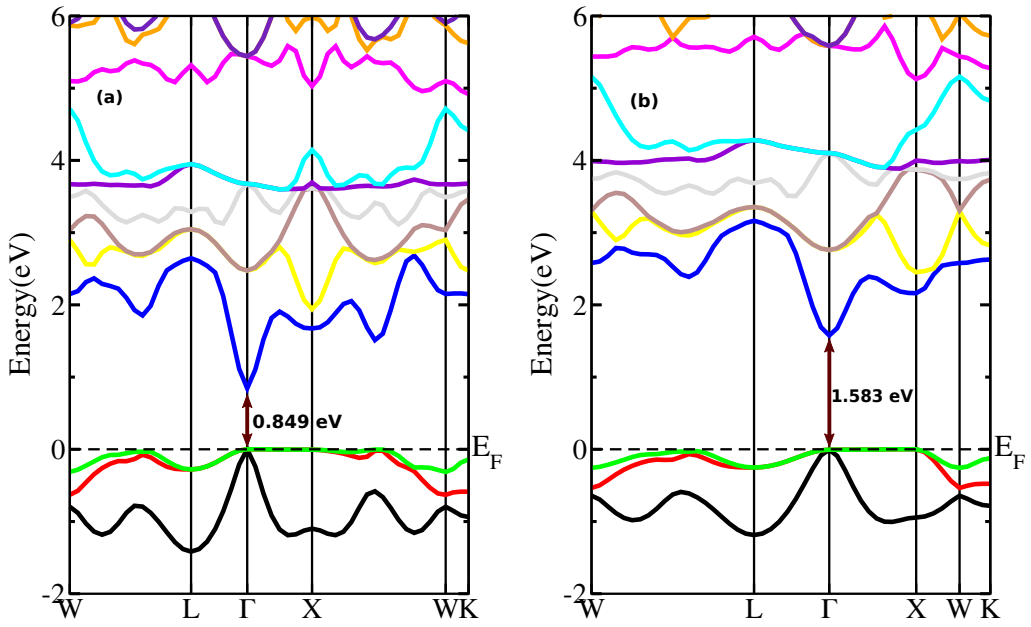


Figure 3.3: Band Structure of RbSrBi for (a) PBE-GGA and for (b) TB-mBJ potential.

3.3.2 Density of states

The density of states (DOS) represents the number of available states at a particular energy level that electrons can occupy, or the number of electron states per unit volume per unit energy. We use density of states (DOS) and partial density of states (PDOS) to explain the energy levels of electrons near fermi energy level. This allows us to identify a material as an insulator, a semiconductor, or a conductor. For the study of electronic properties of materials, it is necessary to calculated the total density of state (TDOS) and partial density states (PDOS). The corresponding total and partial density of states for RbSrBi are illustrated in figure 3.4(a-d).

In this system, in valence band (VB), Bi energy bands are dominated and in conduction band (CB), hybridization occurs between Rb and Sr at figure 3.4(a). In the figure, the black vertical dashed line at 0 eV represents E_F (fermi energy level). In

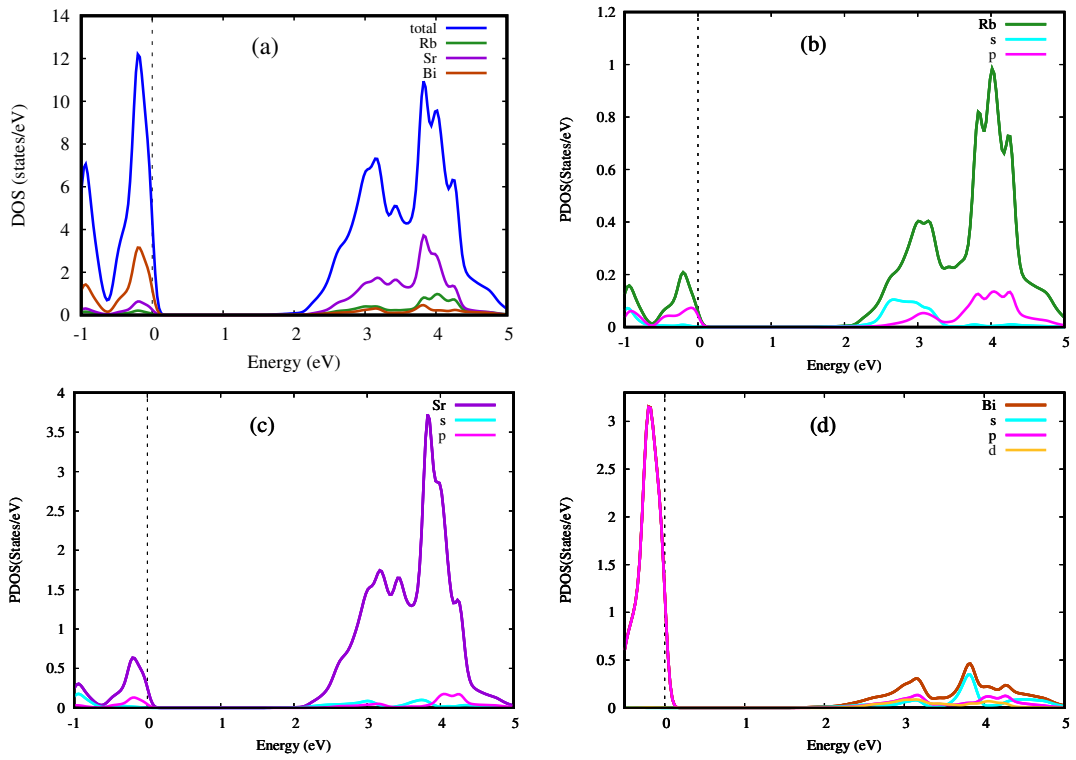


Figure 3.4: (a) Total density of states (TDOS) of RbSrBi and partial density of states (PDOS) of (b) Rb (c) Sr and (d) Bi atoms.

figure 3.4(b), the conduction band shows a prominent peak centered around 4 eV, dominated by Rb s-states where the smaller peak around 2 eV indicates a secondary contribution to the conduction band, likely from p-states. The valence band appears to be dominated by Rb s-states, while the conduction band is primarily composed of Rb s-states with some contributions from p-states. Similarly, in figure 3.4(c), Sr atom has almost same contribution for Valence band and conduction band. In figure 3.4(d), the conduction band shows a prominent peak centered around 4 eV, dominated by Bi p states. There are smaller contributions from s-states around 3.5 eV and d-states around 2.5 eV. The DOS plot suggests a strong p-state character in both the valence and conduction bands of this material. The valence band is dominated by Bi p-states, while the conduction band is also primarily composed of Bi p-states with some contributions from s-states and d-states.

The electronic structure of RbSrBi reveals a band structure indicative of a semiconductor, with a small gap near the Fermi level (E_F). However, the density of states (DOS) shows a significant presence of states at E_F, primarily due to Bi con-

tributions. This suggests semi-metallic behavior, where the valence band overlaps slightly with E_F. These results indicate that RbSrBi is not a typical semiconductor but exhibits more complex electronic properties, which could be advantageous for electronic applications.

3.4 Electron density

Electron density is the measure of the probability of finding electron in a specific location around an atom or molecule. Charge density is the measure of electric charge per unit area of a surface, or per unit volume of a body or field, which describes how much charge is stored in a particular field. Electron density and its distribution plot can be used to investigate the bonding properties of the compound.

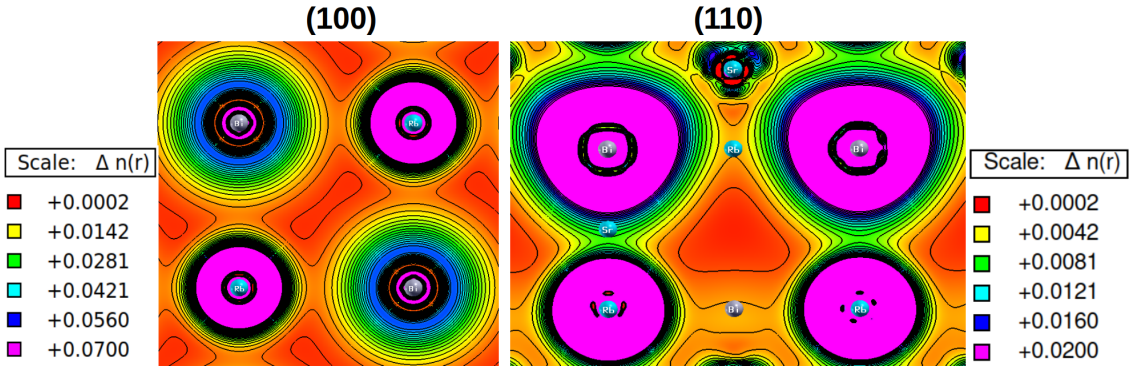


Figure 3.5: Electron density of RbSrBi for (100) and (110) plane.

Figure 3.5 represent the charge density along the crystallographic planes (100) and (110) respectively for RbSrBi. For (100) plane, high electron density regions are localized around Bi atoms, while Rb atoms display lower, more delocalized densities. The presence of moderate electron density overlap between adjacent atoms suggests partial covalent bonding characteristics. However, the well-separated density regions around each atom also indicate a strong ionic contribution to the bonding. These features collectively reveal a mixed ionic-covalent bonding nature within the crystal structure, influenced by the electronic properties of Rb and Bi. The another picture illustrates the electron density distribution of the RbSrBi structure along the (110) crystallographic plane. High electron density regions, shown by dark contours (black

and purple), are localized around the Bi atoms, indicating strong electron localization due to their heavy atomic character. In contrast, Rb and Sr atoms exhibit lower electron density, suggesting more delocalized electronic states. Sr atoms show slightly higher electron accumulation compared to Rb, consistent with their greater electronegativity and smaller atomic radius. The smooth electron density gradients between adjacent atoms reveal regions of electron sharing, indicating predominantly ionic bonding with minor covalent character, which stabilizes the crystal structure.

3.5 Optical properties

In order to understand the optical properties of half-Heusler compound, we have studied the dielectric function (ϵ), absorption coefficient (A), conductivity, reflectivity (R), and refractive index (η) of RbSrBi. The optical properties of the half-Heusler compound were investigated using the TB-mBJ method within the photon energy range of 0 to 12 eV.

3.5.1 Dielectric function

Dielectric function, $\epsilon(\omega)$ determines how light interacts with a substance, influencing phenomena such as refraction, reflection, absorption, and dispersion. There are two parts of dielectric function, which are imaginary dielectric function and real dielectric function. The mathematical formula for dielectric function as given by Ehrenreich and Cohen's is, [49]

$$\epsilon(\omega) = \epsilon_1(\omega) + i\epsilon_2(\omega) \tag{3.1}$$

where, (ϵ_1) and (ϵ_2) are the real and imaginary part of the dielectric function. Real dielectric function ($\epsilon_1(\omega)$) represents the degree of polarization of a material when it placed into an electric field and imaginary dielectric function ($\epsilon_2(\omega)$) represents the energy dissipation aptitude of a dielectric material. The dielectric function is physically analogous to the absolute permittivity in terms of its relationship to the space materials. The imaginary part of dielectric function is directly associated with the materials band gap and explains the absorption nature of the compound. $\epsilon_1(\omega)$

and $\epsilon_2(\omega)$ are related through Kramer–Kronig relation:

$$\epsilon_1(\omega) = 1 + \frac{2}{\pi} P \int_0^{\infty} \frac{\omega' \epsilon_2(\omega')}{\omega'^2 - \omega^2}, \tag{3.2}$$

$$\epsilon_2(\omega) = \frac{e^2 h}{\pi m^2 \omega^2} \sum_{v,c} \int_{BZ}^{\infty} |M_{cv}|^2 \delta[\omega_{cv}(k) - \omega] d^3k, \tag{3.3}$$

where P and k represent the principal quantum number and wave vector, respectively. Here, h is Planck's constant, ω is the angular frequency, and M is the molar mass of the carriers. The $\epsilon_1(\omega)$ and $\epsilon_2(\omega)$ enable us to compute other optical parameters such as absorption coefficient $\alpha(\omega)$, optical conductivity $\sigma(\omega)$, reflectivity R(ω), refractive index n(ω) as follows

$$\alpha(\omega) = \sqrt{2} \frac{\omega}{c} \left\{ \sqrt{\epsilon_1^2(\omega) + \epsilon_2^2(\omega)} - \epsilon_1(\omega) \right\}^{\frac{1}{2}} \tag{3.4}$$

$$n(\omega) = \left[\frac{\sqrt{\epsilon_1^2(\omega) + \epsilon_2^2(\omega)} + \epsilon_1(\omega)}{2} \right]^{\frac{1}{2}} \tag{3.5}$$

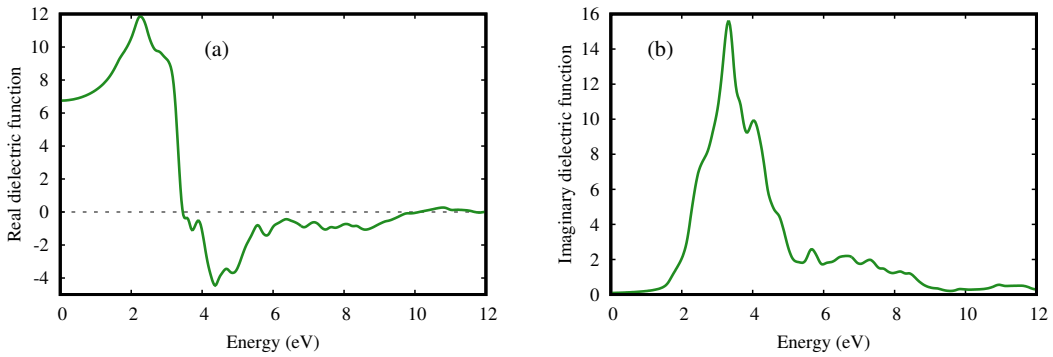


Figure 3.6: (a) Real dielectric function and (b) Imaginary dielectric function of RbSrBi.

The figures 3.6(a) and 3.6(b) represent the real and imaginary dielectric functions of RbSrBi compound. The positive half is concerned with electromagnetic wave propagation, while the negative half is concerned with electromagnetic wave absorption. As a result, the larger the static value of $\epsilon_1(0)$, the smaller the magnitude

of the band gap formed. The positive part of $\epsilon_1(\omega)$indicates that RbSrBi conducts at low energy levels, while the negative part of $\epsilon_1(\omega)$ indicates that it is insulating at high energy levels. $\epsilon_1(\omega)$ begins to exhibit negative values at 3.7 eV and reaches its maximum negative values at 4.5 eV. The positive peak value is around 2.5 eV. In figure 3.6(b), RbSrBi represents its peak value around 3.8 eV. Peaks represent charge carriers shifting from filled to empty bands. As energy increases, $\epsilon_2(\omega)$ begins to decrease and approaches almost zero at around 12 eV.

3.5.2 Absorption coefficient

Absorption of photons occur during the transition of an electron from an unoccupied to an occupied state. Figure 3.7(a) represents the absorption coefficient of RbSrBi. It can be observed in figure 3.7(b) that absorptivity increases progressively in the infrared and visible region, reaches a maximum at 4.4 eV (ultra-violet region), and decreases with increasing energy values. The absorption peak demonstrates that this material can absorb photons in both the ultra-violet and visible ranges.

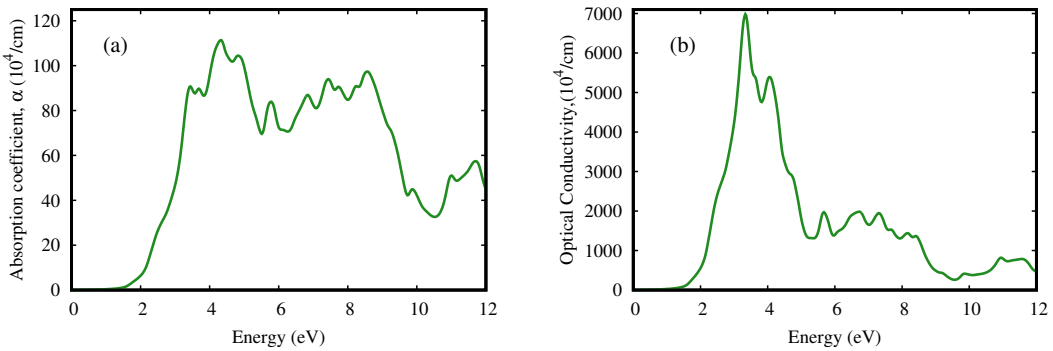


Figure 3.7: (a) Absorption coefficient (b) Optical conductivity of RbSrBi of RbSrBi.

3.5.3 Optical conductivity

Optical conductivity is a material property that describes the interaction between the induced current density in the material and the magnitude of the inducing electric field for arbitrarily selected frequencies. The optical conductivity along with its energy is illustrated in figure 3.7(b). From the optical conductivity curve, it is obvious that conductivity increases as energy increases. From the optical conductivity

curve, it is obvious that conductivity increases as energy increases. The maximum conductivity peaks are obtained at 3.7 eV. Then optical conductivity begins to decrease. The optical curve reveals that the absorbed light spent the conductivity in the UV region.

3.5.4 Reflectivity

Generally, we know that reflection is the change in direction of wavefront at an interface between two different media with different so that the wavefront returns into the medium from which it originated. Optical reflectivity is another parameter which plays a vital role in shifting electron from valance band to the conduction band. The amount of energy absorbed, reflected, and transmitted by a material is equal to the incident photon energy. Estimating the absorbance and transmittance of the substance on which light is incident it is possible to compute the total amount of ray incident on the surface of a semiconductor.

$$A + R + T = 1 \tag{3.6}$$

where, A, R, and T represents the absorbance, reflectance, and transmittance of a material respectively. The optical reflectivity of estimated half-Heusler compound is shown in figure 3.8(a). From the figure 3.8(a), we can see that the maximum peak value is in the range of 9-10 eV which is ultra-violet region.

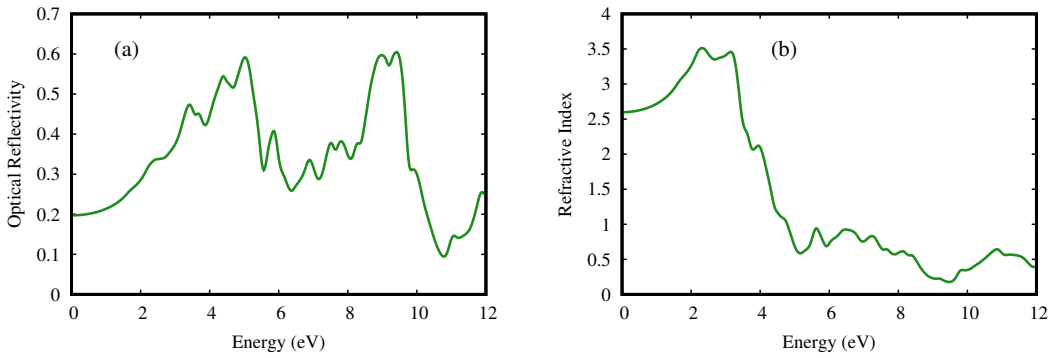


Figure 3.8: (a) Optical Reflectivity and (b) Refractive index of RbSrBi.

3.5.5 Refractive index

Generally, we know that the refractive index means how fast light travels through the material. The refractive index is another important physical quantity that describes the optical properties of any given material. The refractive index of a meterial, gives how much refractive indices are inversely related to the bandgap, if refractive index increases corresponding bandgap decreases, refractive index vs energy curve represent in figure 3.8(b). It can be seen that in the low energy limit, the refractive index has a high value. The maximum peak value is in the range of 2.4 eV which is visible region.

3.6 Thermoelectric characteristics

Thermal energy can be converted into electrical energy in thermoelectric material by using the potential difference produced by the heat gradient during energy transmission [50, 51]. The thermoelectric properties have been calculated for RbSrBi half-Heusler compound using BoltzTraP code. We determined the transport coefficients such as the Seebeck coefficient (S), electrical conductivity (σ/τ), electronic thermal conductivity (κ_e/τ), power factor ($S^2\sigma/\tau$) and dimensionless figure of merit (ZT) as a function of temperature, combined in a compressed form as, [52]

$$ZT = \frac{S^2\sigma T}{k} \tag{3.7}$$

Electrical conductivity defines the concentration of free electron. The moibility of charge carriers estimated in terms of the electric conductivity, which was plotted in the temperature range 100-1000 K, as depict in figure 3.9(a).

Another part of conductivity comes from lattice vibration and thermal agitation, which is the thermal conductivity. Thermal conductivity describes the transportation through a material as the materials atom are constantly moving in rotational, translational or vibrational motion. The variation of atoms is responsible for generating heat or thermal energy in a material. The rate of increase in electronic thermal conductivity is faster than the electrical conductivity. That means, at higher tem-

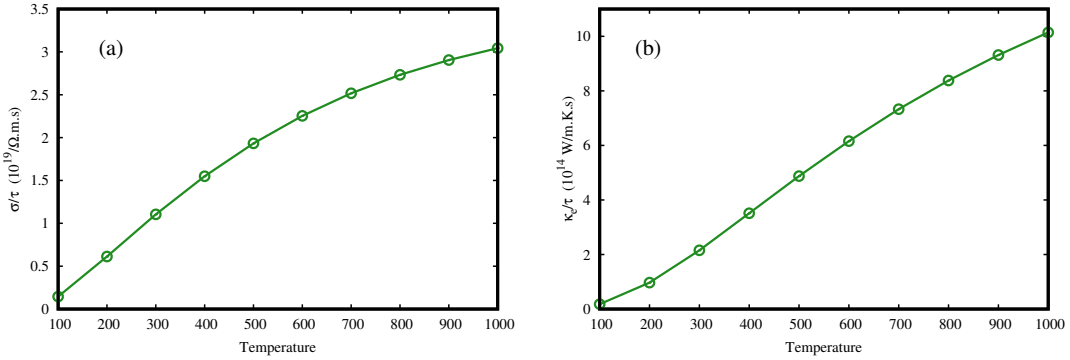


Figure 3.9: (a) Electrical Conductivity (b) Electronic Thermal Conductivity of RbSrBi.

perature more lattice vibrations are generated. Figure 3.9(b) showed the electronic thermal conductivity of RbSrBi. From the figure electronic thermal conductivity increased with increasing pressure against temperature.

The Seebeck coefficient measure the magnitude of induced change in voltage by applying the change in temperature, which can be seen in the mathematical form,

$$S = \frac{\mu \nabla V}{\nabla T} \tag{3.8}$$

Therefore, the potential difference induced by the temperature gradient is called the Seebeck coefficient. The Seebeck coefficient (S) is used to find the potential difference that can occur between the contacts of dissimilar metals as a function of temperature change, which is shown in figure 3.10(a). From figure, we can see that Seebeck coefficient decreased with rising temperature.

The power factor is another thermoelectric parameter that is used to determine the thermoelectric performance of any material and this is calculated by the expression PF $=\sigma S^2$. Power factor represents how effectively the generated power will be used by the compound. Power factor increases with an increase of temperature, which demonstrates suitability of this material for high temperature applications. The power factor of RbSrBi displays in figure 3.10(b) that rising with applied temperature. Here the maximum value at 700 K.

Another important factor to estimate the actual thermoelectric efficiency of the

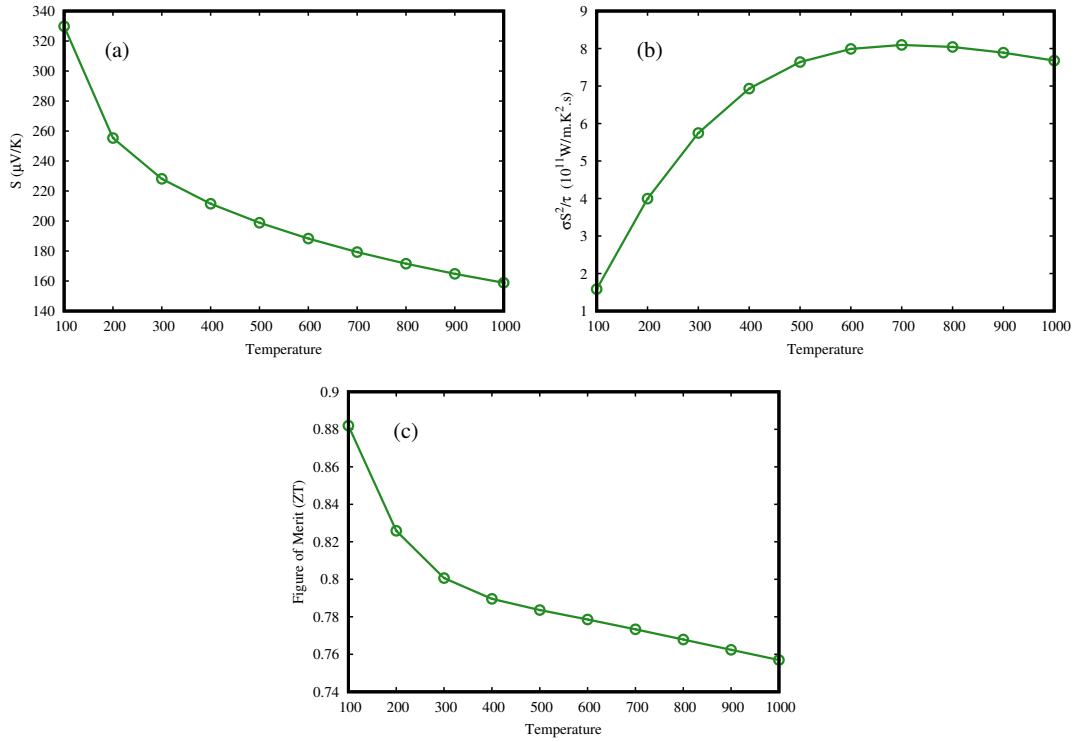


Figure 3.10: (a) Seebeck coefficient (b) Power factor and (c) Figure of merit and of RbSrBi.

studied compound, a dimensionless parameter labeled as figure of merit i.e., ZT = $(\sigma S^2/\kappa)$ was used to assess their thermoelectric performance. The parameters σ, S, and κ represents electrical conductivity, Seebeck coefficient and thermal conductivity, respectively. Figure of merit represents how efficiently the generated heat will be converted into electricity. The figure of merit (ZT) is used to measure the materials quality for thermal devices. The efficiency of a thermoelectric material depends on the figure of merit. For high efficiency, high electrical conductivity and low electronic thermal conductivity is required. The variation of figure of merit (ZT) for the RbSrBi half-Heusler compound in the temperature range 100-1000 K, which is illustrate in Figure 3.10(c). For RbSrBi, the value of figure of merit decreases with increasing temperature.

Chapter 4

Conclusion

In this project, the structural, optoelectronic, and thermoelectric characteristics of RbSrBi half-Heusler compound were studied using the Full Potential Linear Augmented Plane Wave (FP-LAPW) method based on Density Functional Theory (DFT) implemented in WIEN2k code. The findings showed that the material is stable in a cubic structure with a lattice constant of 8.12 Å. The electronic band structure showed that RbSrBi is a direct bandgap semiconductor, with bandgap values of 0.849 eV using PBE-GGA and 1.583 eV using TB-mBJ potential. The density of states analysis revealed that the Bi-p orbitals mainly contribute to the states near the fermi level. The charge density study indicated a mixture of ionic and covalent bonding. The optical properties showed strong absorption in the visible and ultraviolet regions. A high refractive index and large dielectric constant were also observed, suggesting that the material could be used in optical and photovoltaic devices. The thermoelectric properties were calculated using BoltzTraP code. The material showed a good Seebeck coefficient, suitable electrical conductivity, and reasonable thermal conductivity. The figure of merit (ZT) values suggested good thermoelectric performance at high temperatures. The overall investigation of the RbSrBi half-Heusler compound highlights its potential for sustainable applications in optoelectronic and thermoelectric power generation.

Bibliography

[1] Hayati Mamur and Rasit Ahıska. A review: Thermoelectric generators in renewable energy. *International Journal of Renewable Energy Research*, 4(1):128–136, 2014.

[2] Jarman T Jarman, Essam E Khalil, and Elsayed Khalaf. Energy analyses of thermoelectric renewable energy sources. *Open Journal of Energy Efficiency*, 2013, 2013.

[3] Joseph R Sootsman, Duck Young Chung, and Mercouri G Kanatzidis. New and old concepts in thermoelectric materials. *Angewandte Chemie International Edition*, 48(46):8616–8639, 2009.

[4] Heng Wang, Yanzhong Pei, Aaron D LaLonde, and G Jeffery Snyder. Material design considerations based on thermoelectric quality factor. *Thermoelectric Nanomaterials: Materials Design and Applications*, pages 3–32, 2013.

[5] Jiaqing He, Mercouri G Kanatzidis, and Vinayak P Dravid. High performance bulk thermoelectrics via a panoscopic approach. *Materials Today*, 16(5):166–176, 2013.

[6] M Upadhyay Kahaly and Udo Schwingenschlögl. Thermoelectric performance enhancement of SrTiO 3 by Pr doping. *Journal of Materials Chemistry A*, 2(27):10379–10383, 2014.

[7] Joseph R Sootsman, Duck Young Chung, and Mercouri G Kanatzidis. New and old concepts in thermoelectric materials. *Angewandte Chemie International Edition*, 48(46):8616–8639, 2009.

[8] H Julian Goldsmid. Improving the thermoelectric figure of merit. *Science and Technology of Advanced Materials*, 22(1):280–284, 2021.

[9] Debidatta Behera, Ramesh Sharma, Hamid Ullah, Hafiza Sumaira Waheed, and SK Mukherjee. Electronic, optical, and thermoelectric investigations of zintl phase AAg_2Se_2 (A= Sr, Ba) compounds: A first-principle approach. *Journal of Solid State Chemistry*, 312:123259, 2022.

[10] Arash Mehdizadeh Dehkordi, Mona Zebarjadi, Jian He, and Terry M Tritt. Thermoelectric power factor: Enhancement mechanisms and strategies for higher performance thermoelectric materials. *Materials Science and Engineering: R: Reports*, 97:1–22, 2015.

[11] Debidatta Behera, Ahmed Azzouz-Rached, Abdessalem Bouhenna, Mostafa M Salah, Ahmed Shaker, and Sanat Kumar Mukherjee. First-principles studies on the physical properties of the half heusler rbnbcd and rbnbzn compounds: a promising material for thermoelectric applications. *Crystals*, 13(4):618, 2023.

[12] Jan-Willem G Bos and Ruth A Downie. Half-heusler thermoelectrics: a complex class of materials. *Journal of Physics: Condensed Matter*, 26(43):433201, 2014.

[13] Tanja Graf, Frederick Casper, Jürgen Winterlik, Benjamin Balke, Gerhard H Fecher, and Claudia Felser. Crystal structure of new heusler compounds. *Zeitschrift für anorganische und allgemeine Chemie*, 635(6-7):976–981, 2009.

[14] Long Chen, Xiaoyu Zeng, Terry M Tritt, and S Joseph Poon. Half-heusler alloys for efficient thermoelectric power conversion. *Journal of Electronic Materials*, 45:5554–5560, 2016.

[15] Yufeng Wu, Bo Wu, Zhenyi Wei, Zeyou Zhou, Chunfeng Zhao, Yuanpeng Xiong, Shushi Tou, Shangjin Yang, Baiyang Zhou, and Yanqun Shao. Structural, half-metallic and elastic properties of the half-heusler compounds NiMnM (M= Sb, As and Si) and irmnas from first-principles calculations. *Intermetallics*, 53:26–33, 2014.

[16] Zhou Yi, Pei-Na Deng, Li-Li Zhang, and Hua Li. Dynamic behaviors of water contained in calcium–silicate–hydrate gel at different temperatures studied by quasi-elastic neutron scattering spectroscopy. *Chinese Physics B*, 25(10):106401, 2016.

[17] Thomas Gruhn. Comparative ab initio study of half-heusler compounds for optoelectronic applications. *Physical Review B—Condensed Matter and Materials Physics*, 82(12):125210, 2010.

[18] S Kacimi, H Mehnane, and A Zaoui. I–ii–v and i–iii–iv half-heusler compounds for optoelectronic applications: Comparative ab initio study. *Journal of Alloys and Compounds*, 587:451–458, 2014.

[19] Yasemin O Ciftci and Subhendra D Mahanti. Electronic structure and thermoelectric properties of half-heusler compounds with eight electron valence count—KScX(X= C and Ge). *Journal of Applied Physics*, 119(14), 2016.

[20] Deepika Shrivastava, Nikita Acharya, and Sankar P Sanyal. Investigation of thermoelectricity in KScSn half-heusler compound. In *AIP Conference Proceedings*, volume 1953. AIP Publishing, 2018.

[21] Deepika Shrivastava and Sankar P Sanyal. Theoretical study of structural, electronic, phonon and thermoelectric properties of KScX (X= Sn and Pb) and KYX (X= Si and Ge) half-heusler compounds with 8 valence electrons count. *Journal of Alloys and Compounds*, 784:319–329, 2019.

[22] Qiulin Yuan, Minping Zhang, Gongping Zheng, and Guangtao Wang. Effective spin-orbital coupling determined topological properties of half-heusler compounds XYZ (X= Li, Na, K; Y= Ag, Au; Z= S, Se, Te). *Journal of Alloys and Compounds*, 963:171070, 2023.

[23] D Shobana Priyanka, G Venkatesh, M Srinivasan, G Palanisamy, and P Ramasamy. Half metallic heusler alloys xmnge (X= Ti, Zr, Hf) for spin flip and thermoelectric device application–material computations. *Materials Science in Semiconductor Processing*, 159:107367, 2023.

[24] A Saim, F Belkharroubi, FZ Boufadi, I Ameri, LF Blaha, A Tebboune, MN Belkaid, W Belkilali, M Ameri, Y Al-Douri, et al. Investigation of the structural, elastic, electronic, and optical properties of half-heusler CaMgZ (Z= C, Si, Ge, Sn, Pb) compounds. *Journal of Electronic Materials*, 51(7):4014–4028, 2022.

[25] Muhammad Atif Sattar, Mehreen Javed, Najwa Al Bouzieh, Maamar Benkraouda, and Noureddine Amrane. First-principles investigation on the novel half-heusler VXTe (X= Cr, Mn, Fe, and Co) alloys for spintronic and thermoelectric applications. *Materials Science in Semiconductor Processing*, 155:107233, 2023.

[26] Soumya Ranjan Mishra, Anirudha Karati, Sanyukta Ghosh, Ramesh Chandra Mallik, Rajashekhara Shabadi, PS Sankara Rama Krishnan, Satyesh Kumar Yadav, RV Ramanujan, and BS Murty. Lowering thermal conductivity in thermoelectric Ti_{2-x}NiCoSnSb half heusler high entropy alloys. *Journal of Materials Science*, 58(26):10736–10752, 2023.

[27] Y Rached, M Caid, H Rached, M Merabet, S Benalia, S Al-Qaisi, L Djoudi, and D Rached. Theoretical insight into the stability, magneto-electronic and thermoelectric properties of XCrSb (X: Fe, Ni) half-heusler alloys and their superlattices. *Journal of Superconductivity and Novel Magnetism*, 35(3):875–887, 2022.

[28] Peter Blaha, Karlheinz Schwarz, Georg KH Madsen, Dieter Kvasnicka, Joachim Luitz, et al. Wien2k. *An augmented plane wave+ local orbitals program for calculating crystal properties*, 60(1), 2001.

[29] Peter Blaha, Karlheinz Schwarz, Fabien Tran, Robert Laskowski, Georg KH Madsen, and Laurence D Marks. Wien2k: An apw+ lo program for calculating the properties of solids. *The Journal of Chemical Physics*, 152(7), 2020.

[30] Pierre C Hohenberg and James S Langer. Walter kohn, 2016.

[31] Michael P Marder. *Condensed Matter Physics*. John Wiley & Sons, 2010.

[32] David J Griffiths and Darrell F Schroeter. *Introduction to Quantum Mechanics*. Cambridge university press, 2019.

[33] Wolfram Koch and Max C Holthausen. *A chemist's guide to density functional theory*. John Wiley & Sons, 2015.

[34] Erwin Schrödinger. An undulatory theory of the mechanics of atoms and molecules. *Physical Review*, 28(6):1049, 1926.

[35] Klaus Capelle. A bird's-eye view of density-functional theory. *Brazilian Journal of Physics*, 36:1318–1343, 2006.

[36] Walter Kohn. Nobel lecture: Electronic structure of matter—wave functions and density functionals. *Reviews of Modern Physics*, 71(5):1253, 1999.

[37] Pierre Hohenberg and Walter Kohn. Inhomogeneous electron gas. *Physical Review*, 136(3B):B864, 1964.

[38] John A Pople, Peter MW Gill, and Benny G Johnson. Kohn—sham density-functional theory within a finite basis set. *Chemical Physics Letters*, 199(6):557–560, 1992.

[39] Rüdiger Bauernschmitt and Reinhart Ahlrichs. Stability analysis for solutions of the closed shell kohn–sham equation. *The Journal of Chemical Physics*, 104(22):9047–9052, 1996.

[40] John P Perdew, Kieron Burke, and Matthias Ernzerhof. Generalized gradient approximation made simple. *Physical Review Letters*, 77(18):3865, 1996.

[41] Peter Blaha, Karlheinz Schwarz, P Sorantin, and SB Trickey. Full-potential, linearized augmented plane wave programs for crystalline systems. *Computer physics communications*, 59(2):399–415, 1990.

[42] Stefaan Cottenier et al. Density functional theory and the family of (l) apw-methods: a step-by-step introduction. *Instituut voor Kern-en Stralingsfysica, KU Leuven, Belgium*, 4(0):41, 2002.

[43] Mumtaz Manzoor, Debidatta Behera, Ramesh Sharma, Muhammad Waqas Iqbal, and SK Mukherjee. First principles insights on the structural, mechanical, dynamical, thermoelectric and thermodynamics properties of novel topological (ScSb) semi-metal. *Materials Science and Engineering: B*, 291:116372, 2023.

[44] Peter Blaha, Karlheinz Schwarz, Georg KH Madsen, Dieter Kvasnicka, Joachim Luitz, et al. Wien2k. *An augmented plane wave+ local orbitals program for calculating crystal properties*, 60(1), 2001.

[45] David Koller, Fabien Tran, and Peter Blaha. Improving the modified becke-johnson exchange potential. *Physical Review B—Condensed Matter and Materials Physics*, 85(15):155109, 2012.

[46] Georg KH Madsen and David J Singh. Boltztrap. a code for calculating band-structure dependent quantities. *Computer Physics Communications*, 175(1):67–71, 2006.

[47] Anubhav Jain, Shyue Ping Ong, Geoffroy Hautier, Wei Chen, William Davidson Richards, Stephen Dacek, Shreyas Cholia, Dan Gunter, David Skinner, Gerbrand Ceder, et al. Commentary: The materials project: A materials genome approach to accelerating materials innovation. *APL Materials*, 1(1), 2013.

[48] Tomoo Katsura and Yoshinori Tange. A simple derivation of the birch–murnaghan equations of state (EOSs) and comparison with EOSs derived from other definitions of finite strain. *Minerals*, 9(12):745, 2019.

[49] Nasir Mehmood and Rashid Ahmad. Structural, electronic, magnetic, and optical properties of half-heusler alloys rumnz (Z= P, As): a first-principle study. *Journal of Superconductivity and Novel Magnetism*, 31:233–239, 2018.

[50] Yingzhi Zhou, Jing Wang, Dongxiang Luo, Dehua Hu, Yonggang Min, and Qifan Xue. Recent progress of halide perovskites for thermoelectric application. *Nano Energy*, 94:106949, 2022.

[51] Sile Hu, Zhilin Ren, Aleksandra B Djurisic, and Andrey L Rogach. Metal halide perovskites as emerging thermoelectric materials. *ACS Energy Letters*, 6(11):3882–3905, 2021.

[52] Sukriti Ghosh and Dinesh C. Gupta. Electronic, magnetic, elastic and thermodynamic properties of Cu_2MnGa. *Journal of Magnetism and Magnetic Materials*, 411:120–127, 2016.